PROCEEDINGS OF THE ROYAL SOCIETY A

FirstCite® e-publishing

Proc. R. Soc. A
doi:10.1098/rspa.2007.0348
Published online

Recent changes in solar outputs and the global mean surface temperature. III. Analysis of contributions to global mean air surface temperature rise

By Mike Lockwood[1,2,*]

[1]*Space Environment Physics Group, School of Physics and Astronomy, University of Southampton, Southampton SO17 1BJ, Hampshire, UK*
[2]*Rutherford Appleton Laboratory, Chilton OX11 0QX, Oxfordshire, UK*

A multivariate fit to the variation in global mean surface air temperature anomaly over the past half century is presented. The fit procedure allows for the effect of response time on the waveform, amplitude and lag of each radiative forcing input, and each is allowed to have its own time constant. It is shown that the contribution of solar variability to the temperature trend since 1987 is small and downward; the best estimate is -1.3% and the 2σ confidence level sets the uncertainty range of -0.7 to -1.9%. The result is the same if one quantifies the solar variation using galactic cosmic ray fluxes (for which the analysis can be extended back to 1953) or the most accurate total solar irradiance data composite. The rise in the global mean air surface temperatures is predominantly associated with a linear increase that represents the combined effects of changes in anthropogenic well-mixed greenhouse gases and aerosols, although, in recent decades, there is also a considerable contribution by a relative lack of major volcanic eruptions. The best estimate is that the anthropogenic factors contribute 75% of the rise since 1987, with an uncertainty range (set by the 2σ confidence level using an AR(1) noise model) of 49–160%; thus, the uncertainty is large, but we can state that at least half of the temperature trend comes from the linear term and that this term could explain the entire rise. The results are consistent with the intergovernmental panel on climate change (IPCC) estimates of the changes in radiative forcing (given for 1961–1995) and are here combined with those estimates to find the response times, equilibrium climate sensitivities and pertinent heat capacities (i.e. the depth into the oceans to which a given radiative forcing variation penetrates) of the quasi-periodic (decadal-scale) input forcing variations. As shown by previous studies, the decadal-scale variations do not penetrate as deeply into the oceans as the longer term drifts and have shorter response times. Hence, conclusions about the response to century-scale forcing changes (and hence the associated equilibrium climate sensitivity and the temperature rise commitment) cannot be made from studies of the response to shorter period forcing changes.

Keywords: solar variability; climate change; solar-terrestrial physics

* Address for correspondence: Rutherford Appleton Laboratory, Chilton OX11 0QX, Oxfordshire, UK (m.lockwood@rl.ac.uk).

Received 27 November 2007
Accepted 14 February 2008

1. Introduction

For a sudden change in the radiative forcing of the Earth's climate system, the global surface air temperature T would approach its new value exponentially with a time constant

$$\tau = C_{\mathrm{H}}/\lambda_{\mathrm{S}} = C_{\mathrm{H}} f T/\{I_{\mathrm{TS}}(1-A)\} = C_{\mathrm{H}} f/\{4\varepsilon\sigma T^3\}, \tag{1.1}$$

where C_{H} is the pertinent ('effective') heat capacity that is in immediate thermal contact with the atmosphere; $\lambda_{\mathrm{S}}^{-1}$ is the equilibrium climate sensitivity; f is the feedback factor ($f>1$ for positive feedback and $f<1$ for negative feedback; note that f is assumed to be independent of T); I_{TS} is the total solar irradiance (TSI); A is the Earth's albedo; ε is the Earth's effective planetary long-wave emissivity (defined as the ratio of global mean long-wave flux emitted at the top of the atmosphere to that for a black body with surface temperature T); and σ is the Stefan–Boltzmann constant (Hansen *et al.* 1985; Schwartz 2007). For the Earth's atmosphere in isolation, C_{H} is so small that the time constant is very short (typically only a few days); however, the very large C_{H} of the Earth's oceans means that the time constant for a complete temperature response of the Earth's coupled ocean–atmosphere system can be several thousand years (e.g. Stouffer 2004). In general, C_{H} refers to the pertinent heat capacity and hence the depth to which the effects of a given change in radiative forcing penetrates into the oceans. Therefore, different changes to the radiation balance can have different response time constants.

In paper 1 (Lockwood & Fröhlich 2007), a response time constant τ longer than the solar cycle length was considered in order to define the underlying trends. This would dampen out the solar cycle (decadal-scale) variations in the Earth's climate response almost completely (Wigley & Raper 1990). Such a long response time of several decades is consistent with many studies using the fully coupled atmosphere–ocean general circulation model (Wetherald *et al.* 2001; Hansen *et al.* 2005; Meehl *et al.* 2005; Wigley 2005).

However, solar cycle variations in the Earth's climate system have been detected. They are strongest in the troposphere at its greatest altitudes (Labitzke & van Loon 1997), but can also be detected in the middle and lower troposphere (e.g. Christy *et al.* 2000; Gleisner 2005; Salby & Callaghan 2006; Svensmark & Friis-Christensen 2007), and such variations are expected from climate model simulations, particularly at low and middle latitudes (Cubasch *et al.* 1997). Several multiple regression studies have shown that solar influences in the temperature record can be separated from other factors (e.g. El Niño Southern Oscillation (ENSO), volcanoes and anthropogenic) by the different spatial patterns of change that they each induce. Haigh (2003) showed that the solar response of tropospheric temperatures is strongest at middle latitudes and not at the Equator, indicating that mechanisms other than direct radiative heating must be involved. Solar cycle variations are weak in surface temperatures (e.g. Crowley & Kim 1996; North & Stevens 1998; Free & Robock 1999; Douglass & Clader 2002; Douglass *et al.* 2004; Lean 2006), but have been detected in ocean surface temperatures as well as air temperatures (White *et al.* 1997). For lower frequency solar variations (periods between decades and centuries), stronger surface temperature responses are detected (Cubasch *et al.* 1997; Drijfhout *et al.* 1999; Rind *et al.* 1999; Tett *et al.* 1999; Stott *et al.* 2001).

Hence, the response of the Earth's surface temperatures to solar variations is frequency-dependent and the Earth's climate system acts as a low-pass filter to reduce, if not completely remove, the faster variations. A review of solar variability effects on the climate system has been given by Haigh (2003).

The detection of, albeit damped, solar cycle variations in the surface air temperature is consistent with recent studies that have given a smaller response time constant to solar variations; for example, Douglass & Clader (2002) and Douglass *et al.* (2004) have reported a response time of $\tau < 1$ year to solar variations and Schwartz (2007) has obtained $\tau = 5 \pm 1$ years for all forcings. These studies agree with a number of results implying short response times to (and rapid recovery from) a variety of rapid radiative changes (Taylor *et al.* 1997; Dickinson & Schaudt 1998; Lindzen & Giannitsis 1998; Santer *et al.* 2001; Alley *et al.* 2003; Wigley *et al.* 2005; Boer *et al.* 2007). These results are not, in most cases, incompatible with the longer response times (as found, for example, by Wetherald *et al.* 2001, Hansen *et al.* 2005, Meehl *et al.* 2005 and Wigley 2005) because the duration of the forcing in many cases is short and the response time of the system is not the same as for sustained forcing changes, such as that from increased well-mixed greenhouse gases, owing to a relative lack of penetration of the thermal signal into the oceans. Understanding the different time constants for different forcings is key to the debate about the future evolution of climate change, as estimates of the constant-composition and constant-emission temperature rise commitments vary from considerable (Wigley 2005) to small (Schwartz 2007).

In paper 2 (Lockwood & Fröhlich in press), it was shown that the conclusion of paper 1, (Lockwood & Fröhlich 2007), that the recent solar trends have been in a direction opposite to that needed to contribute to the rise in global temperatures, is not dependent on the response time constant assumed. In this paper, we quantify the solar contributions to the recent warming with an allowance for the response time constants.

Several studies have analysed the variation of global mean air surface and tropospheric temperatures using a combination of various parameters to quantify inputs into the climate system. For example, Christy & McNider (1994) showed that the lower tropospheric temperatures were strongly influenced by ENSO effects and volcanic effects, and removed their estimated effect to reveal a trend. Santer *et al.* (2001) re-evaluated the trend by making allowance for the fact that the ENSO and volcanic data show some correlation. Michaels & Knappenberger (2000) detected a solar cycle variation in the residual trend and hence Douglass & Clader (2002), Douglass *et al.* (2004) and Lean (2006) included TSI as an additional input in their multivariate fits. These fits used temperature anomaly predictors of the form

$$\Delta T_{\mathrm{P}}(t) = k_{\mathrm{S}} \times S(t, \tau_{\mathrm{S}}) + k_{\mathrm{V}} \times V(t, \tau_{\mathrm{V}}) + k_{\mathrm{E}} \times \Delta E(t, \tau_{\mathrm{E}}) + L(t), \qquad (1.2)$$

where S is the solar input variation; V is the volcanic aerosol effect (quantified by the global mean atmospheric optical depth, AOD); ΔE is the anomaly of energy exchange between the deep ocean and the surface mixing layer (Willis *et al.* 2004), here quantified by the N3.4 ENSO index; L is a linear drift term to allow for anthropogenic greenhouse gas and aerosol emissions (and associated feedbacks); and k_{E}, k_{V} and k_{S} are the appropriate weighting (sensitivity) factors. The input solar variation S has usually been the variation of observed

TSI, although the observed variation in the flux of neutrons, generated by galactic cosmic ray (GCR) bombardment of the atmosphere, has also been used (Svensmark & Friis-Christensen 2007). Note that equation (1.2) contains the implicit assumption that the responses are independent; hence, for example, ΔE is independent of V and S, which is not generally valid (Santer *et al.* 2001; Adams *et al.* 2003). In the form of the temperature predictor given in equation (1.1), the input variations are lagged by best-fit lags τ_S, τ_E and τ_V. However, these lags neither arise from a propagation delay nor from energy being stored in a reservoir and released at some later time—they arise from the response times to the changes in radiative forcing, as discussed above. This means that the time-series would be smoothed and attenuated, not just delayed. Furthermore, the fit has hitherto been constrained by prior choice of the lags and not allowed to explore all parameter space. The present paper repeats the multivariate fits of the previous studies but uses a different temperature anomaly predictor

$$\Delta T_P = k_S \times [S \otimes F(\tau_S)] + k_V \times [V \otimes F(\tau_V)] + k_E \times [\Delta E \otimes F(\tau_E)] + L$$

$$= \Delta T_S + \Delta T_{AOD} + \Delta T_{ENSO} + \Delta T_{LIN}, \tag{1.3}$$

where $\otimes$ represents a convolution and F is a filter response function. This allows us to pass each input variation through a low-pass filter with the relevant time constant τ. The low-pass filter adopted here is a simple 'RC-filter' providing an exponential response. The variables k_E, k_V, k_S, L, τ_S, τ_E and τ_V are then obtained by a best fit of ΔT_P to the observed global mean air surface temperature anomaly ΔT_{OBS}, using the Nelder–Mead simplex (direct search) method (Nelder & Mead 1965; Lagarias *et al.* 1998) to minimize the r.m.s. difference between ΔT_P and ΔT_{OBS}. The search starts from the initial conditions derived from a recursive fit method (where the largest correlation input variation is fitted and then successively removed, using the simpler predictor given by equation (1.2)). Monthly mean data are used and seasonal variations in E and T_{OBS} are reduced by the use of anomaly data. Note that the above procedure finds the optimum fit to the T_{OBS} signal and subsequently (in §3) a noise model will be used to estimate uncertainties; more advanced optimizations find the peak signal/noise ratio but require the use of numerical model simulations to characterize the noise (Stone & Allen 2005).

A note of caution must be introduced at this point about this type of analysis. A chance (but spurious) correlation between two different climate forcings that may appear for a short interval can introduce errors. For example, the chance occurrence of major volcanoes approximately 10 years apart can be interpreted as solar cycle oscillations (North & Stevens 1998) and this can lead to volcanic effects being identified as solar (and vice versa). For this reason, most weight is placed on the fits carried out here using the GCR observations (which cover the longer interval 1953–2007) to quantify the solar input as this reduces the chance of these spurious correlations having an effect. In addition, for this reason, an uncertainty analysis has been presented in §3.

2. Input variations

We use monthly mean data for all inputs to T_P and for the observed global mean air surface temperature anomaly ΔT_{OBS}. The input solar variation S is quantified here using three different time-series data: (i) the PMOD TSI composite

$[I_{TS}]_{PMOD}$, (ii) the ACRIM TSI composite $[I_{TS}]_{ACRIM}$, and (iii) the Climax neutron monitor GCR counts C. Paper 2 (Lockwood & Fröhlich in press) shows that the ACRIM composite is not as accurate as the PMOD and contains a long-term drift that is not found in the TSI reconstructed from solar magnetograms. However, it is included here for comparison with other studies that have made use of it. The use of C is valid for a direct effect of cosmic rays on clouds, or for C being a proxy indicator of TSI, or for a combination of both (see discussion in paper 1 (Lockwood & Fröhlich 2007)). All plots in the present paper make use of C and so the analysis can be extended back to 1953. The results for using the TSI composites for S are also given in tables 1 and 2. The ENSO input is quantified using the N3.4 index anomaly (ΔE), which is based on the observed sea-surface temperature in the centre of the equatorial Pacific El Niño region (Wolter & Timlin 1998; Garrett 2007). The global mean atmospheric optical depth, V, is used to quantify the volcanic input (Ammann *et al.* 2003; Yu *et al.* 2006). The linear variation L accounts for anthropogenic emissions of both greenhouse gases and aerosols. The sum of the radiative forcings due to greenhouse gases over the recent decades has been approximately linear (Hofmann 2006*a*,*b*). The reduction in aerosol emissions has also caused a rise in radiative forcing (Andreae *et al.* 2005). It is advantageous to consider the effects of anthropogenic greenhouse gases and aerosols in one term as their net effect is not a simple combination of the two (Feichter *et al.* 2004). The four input variations (C, V, ΔE and L) are shown in figure 1, along with the HadCRUT3 compilation of the observations ΔT_{OBS} (Brohan *et al.* 2006). The analysis was repeated using the equivalent GISS temperature reconstruction (Hansen *et al.* 1999) and the results (not shown) are almost identical.

3. Results

Figure 2*a* shows the best-fit-predicted global mean surface air temperature anomaly ΔT_P (red line) and compares it with the observed variation ΔT_{OBS} (blue line). Figure 2*b* shows the fit residuals ($\Delta T_{OBS} - \Delta T_P$). The residuals show fluctuations about zero and a weak long-term variation, with persistently positive values in recent years. This may indicate that the use of a linear trend may not be adequate to reproduce an accelerating upward trend, but may also point to the importance of another factor that could be natural internal climate variability. The correlation coefficient is $r = 0.89$, hence $r^2 = 0.79$ of the observed variation is explained. Note that although the predicted values are slightly lower than the observed ones over the last 15 years, the variation is well matched. In particular, ΔT_P, like ΔT_{OBS}, shows peak values in 1998, with lower values in the subsequent years.

Tables 1 and 2 provide the time constants, sensitivities, correlations and trends for this fit, plus the corresponding results for fits obtained using the PMOD and ACRIM TSI composites for S. The correlation coefficient is highest for GCRs ($S = C$) and has a greater significance because it is based on the data for 52 years (as opposed to the 27 years for the TSI variations). It is slightly higher for the PMOD composite (i.e. using $S = [I_{TS}]_{PMOD}$) than that for the ACRIM ($S = [I_{TS}]_{ACRIM}$), but this difference is not statistically significant. The best-fit response time constant for the ENSO variation is $\tau_E \approx 0.4$ year and for

Table 1. Trends from best fits of temperature predictor T_P (given by equation (1.2)) to the observed value T_{OBS} using the GCR flux, the PMOD TSI composite and the ACRIM TSI composite to quantify the solar input. (The years of the correlation, the correlation coefficient r and the r.m.s. difference between T_P and T_{OBS} are also given.)

				trend 1987–2006, $\Delta T/\Delta t$ (10^{-3} K yr^{-1})[a]				
solar input	data years	r	$(\Delta T_{OBS}-\Delta T_P)^2$ (K^2)	solar $\Delta T_S/\Delta t$	ENSO $\Delta T_{ENSO}/\Delta t$	volcanic $\Delta T_{AOD}/\Delta t$	linear L	total $\Delta T_P/\Delta t$
GCR flux	1954–2006	0.887	1.73	−0.26 (−1.3%)	−1.10 (−5.6%)	4.67 (23.9%)	14.70 (75.1%)	18.23 (93.1%)
PMOD TSI	1979–2006	0.878	1.65	−0.71 (−3.6%)	−0.81 (−4.1%)	4.62 (23.6%)	14.78 (75.5%)	18.01 (92.0%)
ACRIM TSI	1979–2006	0.872	1.66	0.61 (3.1%)	−0.99 (−5.1%)	4.64 (23.7%)	14.70 (75.1%)	18.96 (96.9%)

[a]given in brackets as a percentage of the observed trend $\Delta T_{OBS}/\Delta t$=19.57× 10^{-3} K yr^{-1}.

Table 2. The best-fit response time constants and sensitivity factors for the fits given in table 1.

	time constant τ (yr)			sensitivity factors			
solar input	solar τ_S	ENSO τ_E	volcanic τ_V	solar k_S	ENSO k_E	volcanic k_V (K)	linear term L_D (K yr^{-1})
GCR flux	0.83	0.42	0.58	-10.36×10^{-5} K (counts h^{-1})$^{-1}$	9.68×10^{-2}	−2.33	14.70×10^{-3}
PMOD TSI	0.80	0.42	0.58	5.07×10^{-2} K (Wm^{-2})$^{-1}$	9.68×10^{-2}	−2.52	14.78×10^{-3}
ACRIM TSI	0.75	0.41	0.58	5.33×10^{-2} K (Wm^{-2})$^{-1}$	9.68×10^{-2}	−2.53	14.70×10^{-3}

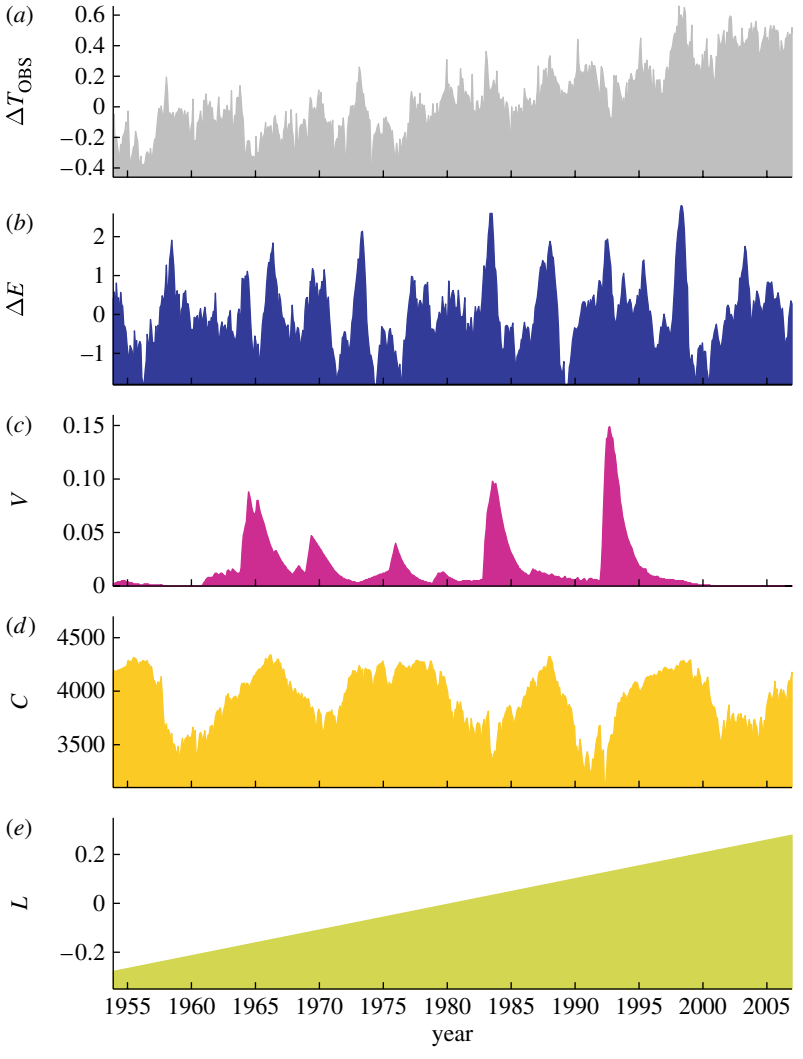

Figure 1. (*a*) The observed global mean air surface temperature anomaly, ΔT_{OBS} (grey, in K). (*b*) The N3.4 El Niño index anomaly, ΔE (blue, in K). (*c*) The global mean atmospheric optical depth (AOD) at 550 nm, V, showing the effects of the Agung, El Chichon and Pinatubo volcanoes (mauve, dimensionless). (*d*) The solar variation, S, quantified by the cosmic ray neutron counts measured at Climax, C (yellow, in h^{-1}). (*e*) A linear rise to include anthropogenic effects (green, in K). All data are monthly means.

the volcanic aerosol forcing is $\tau_V \approx 0.6$ year. In most previous studies, these were given six-month lags. The solar response time $\tau_S \approx 0.8$ year for both the GCR input and the TSI composites. The best-fit sensitivity factors k_E and k_V (for ENSO and volcanic aerosols, respectively) and the linear drift L are almost identical for the three solar inputs. Figure 3 shows the various terms in the predictor ΔT_P, smoothed and lagged for the best-fit time constants and scaled by the sensitivity factors. Note that the dependence of the derived parameters for the ENSO term on the solar forcing variation used may indicate that the two are related statistically, or physically; such a link is not allowed for in the present paper.

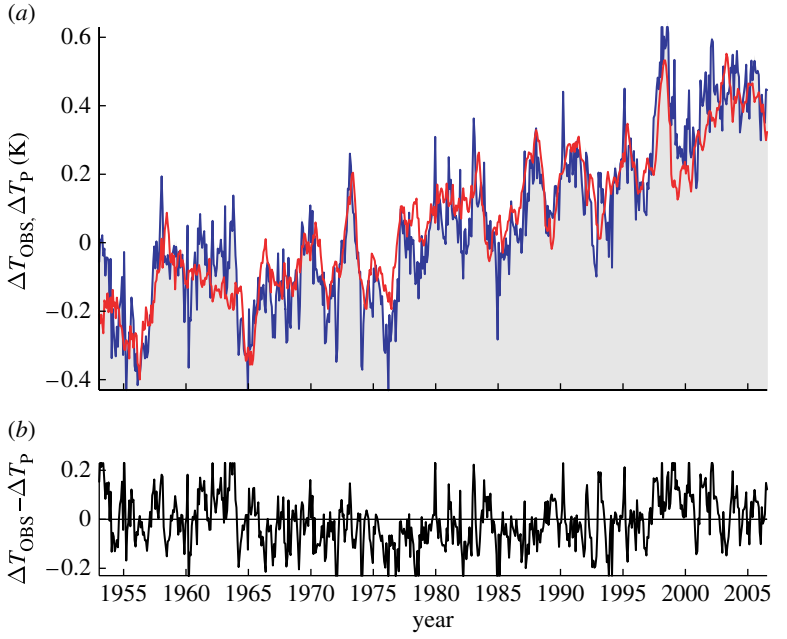

Figure 2. (*a*) The variations of the observed global mean air surface temperature anomaly (ΔT_{OBS}, blue line) and the best multivariate fit (ΔT_P, red line). (*b*) The fit residuals ($\Delta T_{OBS} - \Delta T_P$).

To evaluate the various contributions to recent warming, the average drifts of the contributions to the best-fit ΔT_P (see equation (1.3)) over the data interval 1987–2006 are evaluated and also expressed as a fraction of the observed drift $d\Delta T_{OBS}/dt$ (table 1). The trends are derived using a linear regression fit to the data for the interval considered and are taken since 1987 as that is when paper 1 (Lockwood & Fröhlich 2007) defined the solar input trend to change polarity. The solar drifts are downward (negative) if we use $S = C$ or $S = [I_{TS}]_{PMOD}$, but positive if we use $S = [I_{TS}]_{ACRIM}$. This is not surprising given that paper 2 (Lockwood & Fröhlich in press) shows that the trend in the ACRIM data composite is upward for most of the interval and is downward only relatively recently. Paper 2 (Lockwood & Fröhlich in press) also shows that the main drift in $[I_{TS}]_{ACRIM}$ is an artefact of a pointing direction glitch in the Nimbus HF data. Irrespective of this point, the solar contribution is always small. This is true if we use GCR fluxes or TSI to quantify the solar input. The ENSO trend is also (slightly) negative; in other words, there has been a tendency for La Niña years to outweigh El Niño years towards the end of the period. Again, the effect is small, being approximately 5% of the observed drift in magnitude. The lack of recent major volcanoes has contributed to approximately 24% of the rise. The main cause is that Pinatubo was early in the interval (in 1991) and there has been a recovery from its cooling effect in the subsequent 15 years (Hansen *et al.* 1996). The linear term, added to include anthropogenic effects, accounts for approximately 75% of the total. The sum of these contributions varied between 92 and 97% of the observed rise for the different $S(t)$ adopted.

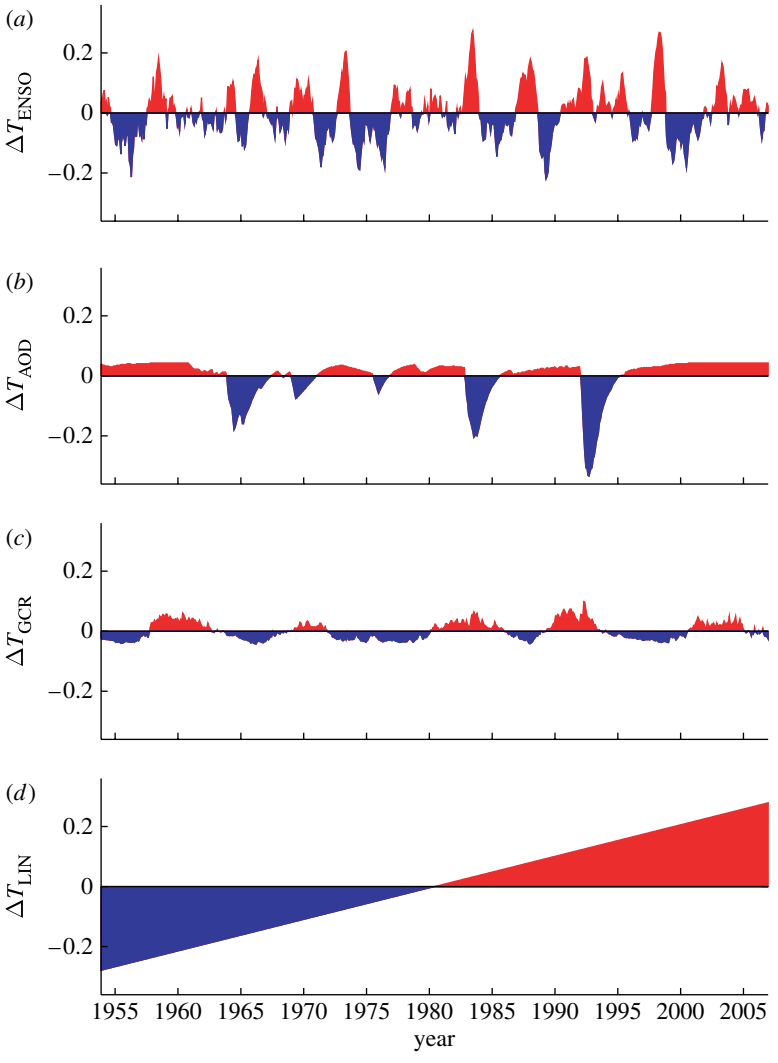

Figure 3. The scaled and filtered variations giving the best-fit ΔT_P shown in figure 2. (*a*) The contribution of deep ocean–surface heat exchange $\Delta T_{ENSO} = k_E \times [\Delta E \otimes F(\tau_E)]$, where k_E is the sensitivity factor and τ_E is the response time constant for ENSO, which is quantified with the N3.4 El Niño index, ΔE. F is the low-pass filter function used. (*b*) The contribution of volcanoes $\Delta T_{AOD} = k_V \times [V \otimes F(\tau_V)]$, where k_V is the sensitivity factor and τ_V is the response time constant for volcanic aerosol effects, which are quantified with the global mean atmospheric optical depth (AOD), V. (*c*) The solar contribution $\Delta T_S = \Delta T_{GCR} = k_S \times [S \otimes F(\tau_S)]$ because the solar variation is represented here by $S = C$, the Climax neutron monitor count rate; k_S and τ_V are the corresponding sensitivity and response time constant. (*d*) The best-fit linear drift ΔT_{LIN}.

4. Comparison of solar and anthropogenic forcings

It is now many years since climate scientists demonstrated that the rise in global mean temperatures was mainly due to anthropogenic effects and the solar contribution was small (e.g. Hansen & Lacis 1990). However, reports of a large,

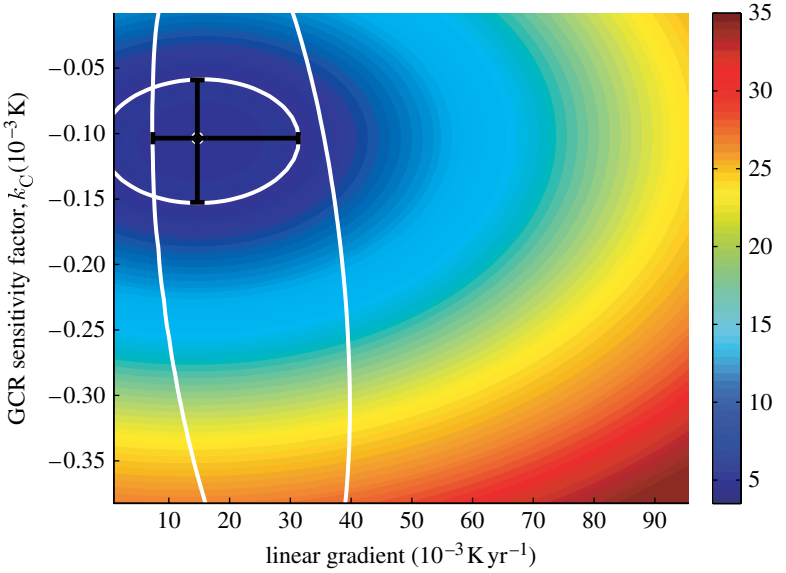

Figure 4. The minimum r.m.s. fit residual $\langle(\Delta T_{\rm OBS} - \Delta T_{\rm P})^2\rangle^{1/2}$ (in K) as a function of the linear gradient L and the sensitivity factor $k_{\rm C}$. The 2σ contour has been highlighted in white. The other white line is the 2σ contour taken from figure 5. The best estimate of L is 14.70×10^3 K yr^{-1} with a minimum of 9.22×10^3 K yr^{-1} and a maximum of 31.33×10^3 K yr^{-1}. The best estimate of the solar sensitivity factor, $k_{\rm C}$, is -10.36×10^{-5} K (counts h^{-1})$^{-1}$ (the minus sign is because an increase in C is associated with a decrease in radiative forcing) with a minimum value of -15.3×10^{-5} K (counts h^{-1})$^{-1}$ and a maximum of -5.9×10^{-5} K (counts h^{-1}) $^{-1}$.

or even dominant, solar contribution persist—although increasingly they are not in the published literature and are in non-reviewed sources such as the media and the Internet. This section compares the uncertainties in the solar and linear terms derived here. To achieve this comparison, the fits were constrained to use pairs of values for the solar forcing sensitivity, $k_{\rm C}$, and the magnitude of the linear term, L. Values of $k_{\rm C}$ ($k_{\rm S}=k_{\rm C}$ because here GCRs are used to quantify the solar input) were varied between 0 and -40×10^{-5} K (counts h^{-1})$^{-1}$ in steps of 0.5×10^{-5} (cf. the best-fit value in table 2 is 10.36×10^{-5}), and the values of L were varied between 0 and 100×10^{-3} K yr^{-1} in steps of 1×10^{-3} K yr^{-1} (cf. the best-fit value in table 2 is 14.70×10^{-3}) and the fit surface studied in this parameter space. For each L–$k_{\rm C}$ pair, the best fit was obtained for the predictor given by equation (1.3) by varying the parameters $k_{\rm E}$, $k_{\rm V}$, $\tau_{\rm S}$, $\tau_{\rm E}$ and $\tau_{\rm V}$. Figure 4 shows the variation of the r.m.s. fit residual $\langle(\Delta T_{\rm OBS}-\Delta T_{\rm P})^2\rangle^{1/2}$ with L and $k_{\rm C}$, and figure 5 shows the corresponding variation of the correlation coefficient between $T_{\rm P}$ and $T_{\rm OBS}$, r. In figure 4, the contour of the r.m.s. residual that is significantly higher than the minimum value (at the 2σ confidence level) has been shown in white. This is computed assuming an autoregressive AR(1) noise model. For this 'red' noise model, the autocorrelation coefficient of monthly $T_{\rm OBS}$ at lag 1 is $\alpha_1=0.928$ and the effective number of independent samples used to compute σ is taken to be $N_{\rm eff}=N(1-\alpha_1)/(1+\alpha_1)=24$ for the $N=643$ data samples available. In figure 5,

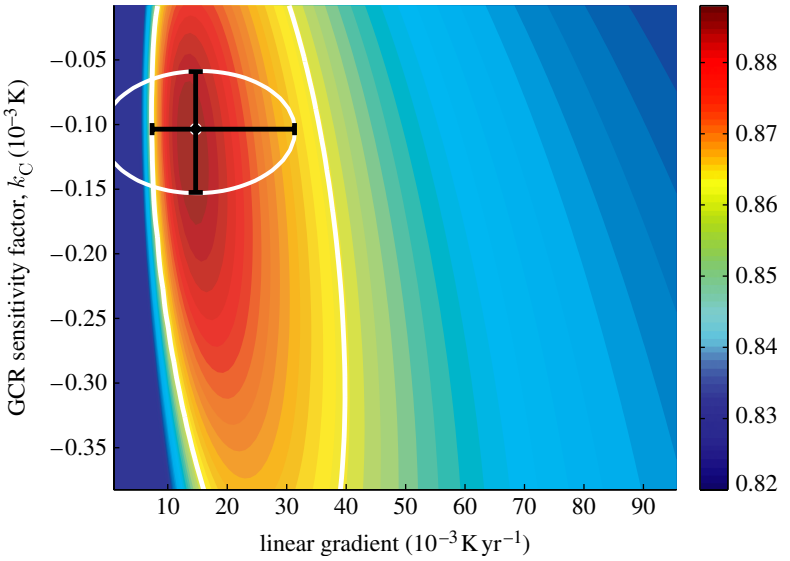

Figure 5. The correlation coefficient between ΔT_{OBS} and ΔT_P, r, as a function of the linear gradient L and the sensitivity factor k_C. The contour of r that is significantly lower than the peak value at the 2σ level (evaluated using Fisher's Z-test) has been highlighted in white. The other white line is the 2σ contour taken from figure 4. The best estimate and error bars are as shown in figure 4.

the weak dependence of the fit on the solar term is reflected by the near-vertical form of the peak in r. The contour of r, which is significantly lower than the peak value (again at the 2σ level), has also been shown in white. This is evaluated using Fisher's Z-test for the significance between two correlation coefficients (Lockwood 2002). The 2σ level contour from figure 5 is also reproduced in figure 4 and vice versa. The best-fit values are shown by the point. The biggest difference in the derived 2σ levels arises because the form of the decadal-scale T_P variation (and hence r) has a weaker dependence on the GCR sensitivity factor k_C than the longer term variation (and hence the r.m.s. fit residual). It can be seen that the uncertainty in the best fit (at the 2σ level) is usually constrained by the fit residuals shown in figure 4. However, figure 5 shows that there is a steep fall-off in the correlation coefficient as the linear drift L is decreased below the best-fit value, such that it sets the uncertainty limit rather than the fit residual. Using a combination of the two we derive the error bars shown in black. The best estimate of L is 14.70×10^{-3} K yr^{-1} with a minimum of 9.22×10^{-3} K yr^{-1} and a maximum of 31.33×10^{-3} K yr^{-1}. The best estimate of the solar sensitivity factor, k_C is -10.36×10^{-5} K (counts h^{-1})$^{-1}$ with a minimum value of -15.3×10^{-5} K (counts h^{-1})$^{-1}$ and a maximum of -5.9×10^{-5} K (counts h^{-1})$^{-1}$. This sensitivity factor has not been quantified in previous studies. We can use the derived fit uncertainties to evaluate the associated uncertainties in the percentage contributions to the total change. For the linear term, the range is 49–160%; thus, the uncertainty is large, but we can state that at least half of the trend comes from the linear term and this term could explain the entire rise. For the solar contribution, the range is -0.7 to -1.9% (with a best estimate of -1.3%).

5. Conclusions and discussion

The analysis presented here quantifies the contributions to recent climate change without recourse to the large and complex numerical models usually used in detection–attribution techniques (see review by Ingram 2006); a lack of understanding of the working and testing of those models often leads sceptics to dismiss their conclusions and hence we have avoided their use here. However, the results presented are in broad general agreement with these more sophisticated detection–attribution studies (e.g. Cubasch *et al.* 1997; North & Stevens 1998; Tett *et al.* 1999; Stott *et al.* 2003; Stone & Allen 2005; Ingram 2006). The only way the solar contribution to the rise in air surface temperatures can be found not to be negative is to use the ACRIM TSI composite. Paper 2 (Lockwood & Fröhlich in press) has presented an analysis of this composite and shown that the drift it gives is erroneous. We show here, using either GCR fluxes or the PMOD TSI composite, that the solar changes have been in the direction opposite to that needed to increase surface air temperatures, as concluded by paper 1 (Lockwood & Fröhlich 2007).

The multivariate fits used to derive this result have been carried out by several sets of authors previously (e.g. Douglass & Clader 2002; Douglass *et al.* 2004; Lean 2006). A number of refinements are introduced here. Firstly, many of the previous analyses used global mean tropospheric temperatures, whereas we here use the mean air surface temperature. Secondly, we use both cosmic ray fluxes and TSI variations to quantify the input solar variation. The biggest difference when compared with previous studies, however, is that the data series are not lagged and then fitted but passed through a low-pass filter to allow for response times. The response times are then derived by the fit procedure. In addition, an analysis of uncertainties has been carried out.

For quasi-periodic variations such as solar forcing, ENSO energy exchange with the deep ocean and volcanic aerosol surface dimming, the response times are found to be less than 1 year. There are approximately 15 El Niño peaks in the 52 years studied, giving a quasi-periodicity of $\sim$3.5 years for the ENSO variation and the response time is found to be 0.4 year. There are five major peaks in the AOD time-series, giving a quasi-periodicity of 10 years and the time constant derived is 0.6 year. Lastly, the mean solar cycle length over the interval is 10.75 years (see paper 1 (Lockwood & Fröhlich 2007)) and the response time is 0.8 year. This suggests that the periodicity of the variation might be a key factor in determining the response times, which are longer for longer period variations. This implies that response times from short (decadal-scale and less)-period fluctuations tell us very little about the response time to continued gradual trends. Autocorrelation techniques have been used to determine the overall response time, for example, Schwartz (2007) derives a value of 5 ± 1 years. However, these will tend to pick out the effect of the relatively short periodicities, rather than slow drifts, and hence may well give smaller values. As discussed in the introduction, the importance of this debate is that the response time (to century-scale changes) sets the amount of warming that we are already committed to, even if greenhouse gas abundances were stabilized.

The results presented here are broadly consistent with the intergovernmental panel on climate change (IPCC) review of current knowledge. The trend for 1987–2006 cannot be compared with the IPCC report as the latter does not

Table 3. A comparison of derived temperature changes and IPCC radiative forcing changes between 1963 and 1993.

	IPCC ΔF (Wm^{-2})	ΔT (K)	IPCC ΔF (%)	ΔT (%)	$\lambda_{\mathrm{S}}'^{-1} = \Delta T/\Delta F$(K W^{-1} m^2)
total	0.50	0.369	100	100	0.74
solar	0.06	0.016	12	4	0.27
volcanic	−0.42	−0.095	−84	−26	0.22
anthropogenic	0.86	0.448	+172	+121	0.52

extend to the later times. Table 3 presents an analysis of the change between 1961 and 1995, which is covered in the IPCC report. Table 6.13 of ch. 6 of the 2007 report (Ramaswamy *et al.* 2007) gives the radiative forcing for 5-year intervals for volcanic aerosols, solar variability and a number of anthropogenic factors (well-mixed greenhouse gases, stratospheric ozone, tropospheric ozone, sulphate pollution, organic carbon and black carbon from fossil fuel and biomass burning). In table 3, the changes in the estimated radiative forcing between 1963 (in fact, a mean for 1961–1965 is used) and 1993 (a mean for 1991–1995) are listed along with the temperature changes associated in the present paper with that radiative forcing (the differences in the means for the same intervals as used in the IPCC report). The rise in the volcanic forcing ΔF_{AOD} and the temperature response ΔT_{AOD} are both negative (because the Pinatubo eruption was close to the end of this interval), but the percentage temperature response (after removal of the internal ENSO signal from the temperature record) is smaller than the percentage forcing change. Determining and constraining climate sensitivity, particularly for long-period variations is uncertain (e.g. Annan & Hargreaves 2006; Hegerl *et al.* 2007). As noted by the IPCC report, instantaneous radiative forcings cannot be used with the temperature change over the same interval to determine climate sensitivities because the temperature changes are not equilibrium responses and the effect of radiative forcings is not a simple addition. The 'apparent' climate sensitivities $\lambda_{\mathrm{S}}'^{-1}$ can be defined as $\Delta T/\Delta F$ (Gregory *et al.* 2002), given in the last column of table 3, and in general will not be equilibrium values as the system has not, in general, had time to fully respond to the changes. However, the previous section finds that the time constant for volcanic and solar variations is $\tau_{\mathrm{S}} = 0.83$ year and $\tau_{\mathrm{V}} = 0.58$ year, respectively; hence, in these cases, the climate sensitivities $[\lambda_{\mathrm{S}}^{-1}]_{\mathrm{S}} = 0.27$ and $[\lambda_{\mathrm{S}}^{-1}]_{\mathrm{V}} = 0.22$ can be regarded as equilibrium values ($\lambda_{\mathrm{S}}'^{-1} = \lambda_{\mathrm{S}}^{-1}$) for which, by equation (1.1), $\tau = C\ \lambda_{\mathrm{S}}^{-1}$. From this, we derive the heat capacity pertinent to solar variations $C_{\mathrm{S}} = \tau_{\mathrm{S}}/[\lambda_{\mathrm{S}}^{-1}]_{\mathrm{S}} = 3.07$ W yr m^{-2} K^{-1}, which corresponds to a depth of 24 m of the ocean surface layer. Likewise, the heat capacity pertinent to volcanic variations C_{V} is $\tau_{\mathrm{V}}/[\lambda_{\mathrm{S}}^{-1}]_{\mathrm{V}} = 2.64$ W yr m^{-2} K^{-1}, which corresponds to a depth of 21 m of the ocean mixing layer. Hence, we find that decadal-scale variations such as solar variations and volcanic cooling only penetrate to depths of approximately 20 m in the ocean, providing small heat capacities, response times and climate sensitivities. Note that time constants of less than 1 year mean that, in general, the responses could depend on season and so, for example, the effects of episodic volcanic eruptions could depend on time of year.

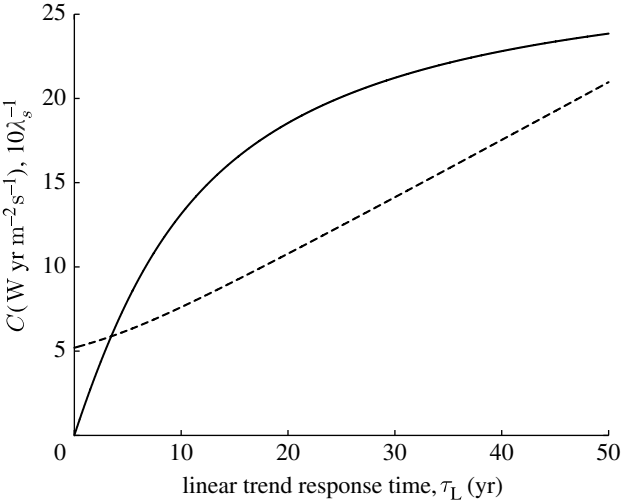

Figure 6. Pertinent heat capacity C (solid line) and $10\lambda_S^{-1}$ (dashed line), where λ_S^{-1} is the equilibrium climate sensitivity, as a function of the linear trend response time constant τ_L.

For a forcing that increases linearly with time such that $\Delta F = \beta t$, the apparent sensitivity is (Gregory *et al.* 2002; Schwartz 2007)

$$\lambda_S'^{-1} = \Delta T/\Delta F = \lambda_S^{-1}[1-(\tau/t)(1-e^{-t/\tau})], \tag{4.1}$$

which tends to the equilibrium sensitivity λ_S^{-1} when $t \gg \tau$. In general, the apparent sensitivity $\lambda_S'^{-1} = \Delta T/\Delta F \leq \lambda_S^{-1}$ and hence the value of $\lambda_S'^{-1} = 0.52$ given in table 1 represents only a lower limit to λ_S^{-1}. For a linear forcing variation, the time constant τ_L cannot be determined using the method applied here to the quasi-periodic ENSO, solar and volcanic variations. Here, we consider a range of the response time constant for the linear anthropogenic term τ_L, varying over the range of 0–50 years. For the study presented in table 3, the apparent climate sensitivity $\Delta T/\Delta F = 0.52$ and $t = 30$ years. From equations (1.1) and (4.1), the variations in the equilibrium climate sensitivity, λ_S^{-1}, and the pertinent heat capacity, C, with the assumed τ_L can be determined. The results are shown in figure 6. If, for example, $\tau_L = 5$ years (as found for all forcings by Schwartz 2007), $t/\tau = 6$, $\lambda_S^{-1} = 0.62$ and $C = 8.06$ W yr m^{-2} K^{-1} (corresponding to an ocean depth of 63 m). The results presented here do not allow us to quantify τ_L and hence λ_S^{-1}, the feedback factor f and the committed temperature rise cannot be determined either. However, given that the response times for the decadal-scale forcing variations (volcanic aerosols and solar) are short, the equilibrium climate sensitivities and pertinent heat capacities are also small (as they penetrate less deeply into the oceans). For the long-term trend, the minimum possible climate sensitivity is at least twice that for these decadal-scale forcing variations. Hence, conclusions drawn using higher frequency variations (decadal timescales and less) will not be valid for longer period trends.

A number of recent publications (e.g. Joshi *et al.* 2003) have noted that the same radiative forcing due to different mechanisms have different effects on global temperatures. As a result, efficacy, E, has been introduced as a measure of

how effective a radiative forcing, from a given anthropogenic or natural mechanism, is in changing the equilibrium global surface air temperature compared with an equivalent radiative forcing from carbon dioxide (so by definition, the efficacy of CO_2 forcing is unity). The effective radiative forcing F_e is $F \times E$, where F is the radiative forcing. Feichter *et al.* (2004) estimate that well-mixed greenhouse gases give an E value of near unity, and direct and indirect aerosol effects give 0.72; they find that the combination of all greenhouse gases and aerosols provide an E value of 0.94. In contrast, Gregory *et al.* (2004) estimate E for solar variations to be in the range of 0.52–0.80. Because the efficacy is defined from the equilibrium response, these numbers are not directly comparable with the apparent sensitivities in table 3; nevertheless, it is interesting to note that table 3 gives the apparent sensitivities for solar and volcanic variations, which are roughly one-half of that for the linear term. As discussed above, the short time constants inferred for the observed solar and volcanic forcing variations indicate that the apparent sensitivities are approximately equal to the equilibrium climate sensitivities ($\lambda_S'^{-1} \approx \lambda_S^{-1}$) for these two forcings, but for the linear term (the combination of anthropogenic greenhouse gases and aerosols), we expect $\lambda_S'^{-1} \leq \lambda_S^{-1}$. Hence, the lower $\lambda_S'^{-1}$ for solar and volcanic effects, compared with the linear term, as indicated in table 3, is qualitatively consistent with previously published efficacy estimates, but quantitatively the difference is greater than that expected.

The author is grateful to the great many scientists who have contributed data to the indices and datasets used in this study and made them available online. The work of mL at the Rutherford Appleton Laboratory is funded by the UK Science and Technology Facilities Council.

References

Adams, B. J., Mann, M. E. & Ammann, C. M. 2003 Proxy evidence for an El Niño-like response to volcanic forcing. *Nature* **426**, 274–278. (doi:10.1038/nature02101)

Alley, R. B. *et al.* 2003 Abrupt climate change. *Science* **299**, 2005–2010. (doi:10.1126/science.1081056)

Andreae, M. O., Jones, C. D. & Cox, P. M. 2005 Strong present-day aerosol cooling implies a hot future. *Nature* **435**, 1187–1190. (doi:10.1038/nature03671)

Annan, J. D. & Hargreaves, J. C. 2006 Using multiple observationally-based constraints to estimate climate sensitivity. *Geophys. Res. Lett.* **33**, L06 704. (doi:06710.01029/02005GL025259)

Ammann, C. M., Meehl, G. A., Washington, W. M. & Zender, C. S. 2003 A monthly and latitudinally varying forcing data set in simulations of the 20th century climate. *Geophys. Res. Lett.* **30**, 1657. (doi: 10.1029/2003GL016875)

Boer, G. J., Stowasser, M. & Hamilton, K. 2007 Inferring climate sensitivity from volcanic events. *Clim. Dyn.* **28**, 481–502. (doi:410.1007/s00382-00006-00193-x)

Brohan, P., Kennedy, J. J., Haris, I., Tett, S. F. B. & Jones, P. D. 2006 Uncertainty estimates in regional and global observed temperature changes: a new dataset from 1850. *J. Geophys. Res.* **111**, D12 106. (doi:10.1029/2005JD006548)

Christy, J. R. & McNider, R. T. 1994 Satellite greenhouse signal. *Nature* **367**, 325–367. (doi:10.1038/367325a0)

Christy, J. R., Spencer, R. W. & Braswell, W. D. 2000 MSU tropospheric temperatures: dataset construction and radiosonde comparisons. *J. Atmos. Oceanic Tech.* **17**, 1153–1170. (doi:10.1175/1520-0426(2000)017<1153:MTTDCA>2.0.CO;2)

Crowley, T. J. & Kim, K.-Y. 1996 Comparison of proxy records of climate change and solar forcing. *Geophys. Res. Lett.* **23**, 359–362. (doi:10.1029/96GL00243)

Cubasch, U., Hegerl, G. C., Voss, R., Waszkewitz, J. & Crowley, T. J. 1997 Crowley simulation of the influence of solar radiation variations on the global climate with an ocean–atmosphere general circulation model. *Clim. Dyn.* **13**, 757–767. (doi:10.1007/s003820050196)

Dickinson, R. E. & Schaudt, K. J. 1998 Analysis of timescales of response of a simple climate model. *J. Climate* **11**, 97–106. (doi:10.1175/1520-0442(1998)011<0097:AOTORO>2.0.CO;2)

Douglass, D. H. & Clader, B. D. 2002 Climate sensitivity of the Earth to solar irradiance. *Geophys. Res. Lett.* **29**, 33 (doi:10.129/2002GL015345)

Douglass, D. H., Clader, B. D. & Knox, R. S. 2004 Climate sensitivity of earth to solar irradiance: update. In *Paper presented at 2004 Solar Radiation and Climate (SORCE) meeting on Decade Variability in the Sun and the Climate, Meredith, New Hampshire, 27–29 October.*

Drijfhout, S. S., Haarsma, R. J., Opsteegh, J. D. & Selten, F. M. 1999 Solar-induced versus internal variability in a coupled climate model. *Geophys. Res. Lett.* **26**, 205–208. (doi:10.1029/1998GL900277)

Feichter, J., Roeckner, E., Lohmannm, U. & Liepert, B. 2004 Nonlinear aspects of the climate response to greenhouse gas and aerosol forcing. *J. Clim.* **17**, 2384–2398. (doi:10.1175/1520-0442(2004)017<2384:NAOTCR>2.0.CO;2)

Free, M. & Robock, A. 1999 Global warming in the context of the little ice age. *J. Geophys. Res.* **104**, 19 057–19 070. (doi:10.1029/1999JD900233)

Garrett, D. 2007 Monthly index values (SST). Climate Prediction Center. See http://www.cpc.ncep.noaa.gov/data/indices/sstoi.indices.

Gleisner, H., Thejll, P., Stendel, M., Kaas, E. & Machenhauer, B. 2005 Solar signals in tropospheric re-analysis data: comparing NCEP/NCAR and ERA40. *J. Atmos. Sol.-Terr. Phys.* **67**, 785–791. (doi:10.1016/j.jastp.2005.02.001)

Gregory, J. M., Stouffer, R. J., Raper, S. C. B., Stott, P. A. & Rayner, N. A. 2002 An observationally based estimate of the climate sensitivity. *J. Clim.* **15**, 3117–3121. (doi:10.1175/1520-0442(2002)015<3117:AOBEOT>2.0.CO;2)

Gregory, J. M., Ingram, W. J., Palmer, M. A., Jones, G. S., Stott, P. A., Thorpe, R. B., Lowe, J. A., Johns, T. C. & Williams, K. D. 2004 A new method for diagnosing radiative forcing and climate sensitivity. *Geophys. Res. Lett.* **31**, L03 205. (doi:10.1029/2003GL018747)

Haigh, J. D. 2003 The effects of solar variability on the Earth's climate. *Phil. Trans. R. Soc. A* **361**, 95–111. (doi:10.1098/rsta.2002.1111)

Hansen, J. & Lacis, A. A. 1990 Sun and dust versus greenhouse gases: an assessment of their relative roles in global climate change. *Nature* **346**, 713–719. (doi:10.1038/346713a0)

Hansen, J., Russell, G., Lacis, A. A., Fung, I., Rind, D. & Stone, P. 1985 Climate response times: dependence on climate sensitivity and ocean mixing. *Science* **229**, 857–859. (doi:10.1126/science.229.4716.857)

Hansen, J., Ruedy, R., Sato, M. & Reynolds, R. 1996 Global surface air temperature in 1995: return to pre-pinatubo level. *Geophys. Res. Lett.* **23**, 1665–1668. (doi:10.1029/96GL01040)

Hansen, J., Ruedy, R., Glascoe, J. & Sato, Mki. 1999 GISS analysis of surface temperature change. *J. Geophys. Res.* **104**, 30 997–31 022. (doi:10.1029/1999JD900835)

Hansen, J. *et al.* 2005 Earth's energy imbalance: confirmation and implications. *Science* **308**, 1431–1435. (doi:1410.1126/science.1110252)

Hegerl, G. C., Zwiers, F. W., Braconnot, P., Gillett, N. P., Luo, Y., Marengo Orsini, J. A., Nicholls, N., Penner, J. E. & Stott, P. A. 2007 Understanding and attributing climate change. In *Climate change 2007: the physical science basis. Contribution of working group i to the fourth assessment report of the intergovernmental panel on climate change* (eds S. Solomon, D. Qin, M. Manning, Z. Chen, M. Marquis, K. B. Averyt, M. Tignor & H. L. Miller), pp. 663–745. Cambridge, UK; New York, NY: Cambridge University Press.

Hofmann, D. J., Butler, J. H., Dlugokencky, E. J., Elkins, J. W., Masarie, K., Montzka, S. A. & Tans, P. 2006*a* The role of carbon dioxide in climate forcing from 1979–2004: introduction of the annual greenhouse gas index. *Tellus B* **58**, 614–619. (doi:10.1111/j.1600-0889.2006.00201.x)

Hofmann, D. J., Butler, J. H., Conway, T. J., Dlugokencky, E. J., Elkins, J. W., Masarie, K., Montzka, S. A., Schnell, R. C. & Tans, P. 2006*b* Tracking climate forcing: the annual greenhouse gas index. *EOS Trans. Am. Geophys. Union* **87**, 509–511. (doi:10.1029/2006E0460002)

Ingram, W. J. 2006 Detection and attribution of climate change, and understanding solar influence on climate. *Space Sci. Rev.* **125**, 199–211. (doi:10.1007/s11214-006-9057-2)

Joshi, M., Shine, K., Ponater, M., Stuber, N., Sausen, R. & Li, L. 2003 A comparison of climate response to different radiative forcings in three general circulation models: towards an improved metric of climate change. *Clim. Dyn.* **20**, 843–854.

Labitzke, K. & van Loon, H. 1997 Signal of the 11-year sunspot cycle in the upper troposphere–lower stratosphere. *Space Sci. Rev.* **80**, 393–410. (doi:10.1023/A:1004907126955)

Lagarias, J. C., Reeds, J. A., Wright, M. H. & Wright, P. E. 1998 Convergence properties of the Nelder–Mead simplex method in low dimensions. *Soc. Ind. Appl. Math. (SIAM) J. Optim.* **9**, 112–147.

Lean, J. 2006 Comment on 'Estimated solar contribution to the global surface warming using the ACRIM TSI satellite composite' by N. Scafetta and B. J. West. *Geophys. Res. Lett.* **33**, L15 701. (doi:10.1029/2005GL025342)

Lindzen, R. S. & Giannitsis, C. 1998 On the climatic implications of volcanic cooling. *J. Geophys. Res.* **103**, 5929–5941. (doi:10.1029/98JD00125)

Lockwood, M. 2002 An evaluation of the correlation between open solar flux and total solar irradiance. *Astron. Astrophys.* **382**, 678–687. (doi:10.1051/0004-6361:20011666)

Lockwood, M. & Fröhlich, C. 2007 Recent oppositely-directed trends in solar climate forcings and the global mean surface air temperature. *Proc. R. Soc. A* **463**, 2447–2460. (doi:10.1098/rspa.2007.1880)

Lockwood, M. & Fröhlich, C. In press. Recent oppositely directed trends in solar climate forcings and the global mean surface air temperature. II. Different reconstructions of the total solar irradiance variation and dependence on response time scale. *Proc. R. Soc. A*. (doi:10.1098/rspa.2007.0347)

Meehl, G. A., Washington, M., Collins, W. D., Arblaster, J. M., Hu, A., Lawrence, E., Buja, L. E., Strand, W. G. & Teng, H. 2005 How much more global warming and sea level rise? *Science* **307**, 1769–1772. (doi:10.1126/science.1106663)

Michaels, P. J. & Knappenberger, P. C. 2000 Natural signals in the MSU lower tropospheric temperature record. *Geophys. Res. Lett.* **27**, 2905–2908. (doi:10.1029/2000GL011833)

Nelder, J. A. & Mead, R. 1965 A simplex method for function minimization. *Comput. J.* **7**, 308–313.

North, G. R. & Stevens, M. 1998 Detecting climate signals in the surface temperature record. *J. Clim.* **11**, 563–577. (doi:10.1175/1520-0442(1998)011<0563:DCSITS>2.0.CO;2)

Ramaswamy, V. *et al.* 2007 Radiative forcing of climate change. In *Climate change 2007: the physical science basis. Contribution of working group 4 to the fourth assessment report of the intergovernmental panel on climate change* (eds S. Solomon, D. Qin, M. Manning, Z. Chen, M. Marquis, K. B. Averyt, M. Tignor & H. L. Miller), pp. 350–416. Cambridge, UK; New York, NY: Cambridge University Press.

Rind, D., Lean, J. & Healy, R. 1999 Simulated time-depended climate response to solar radiative forcing since 1600. *J. Geophys. Res.* **104**, 1973–1990. (doi:10.1029/1998JD200020)

Salby, M. L. & Callaghan, F. P. 2006 Evidence of the solar cycle in the tropical troposphere. *J. Geophys. Res.* **111**, D21 113. (doi:10.1029/2006JD007133)

Santer, B. D. *et al.* 2001 Accounting for the effects of volcanoes and ENSO in comparisons of modelled and observed temperature trends. *J. Geophys. Res.* **106**, 28 033–28 059. (doi:10.1029/2000JD000189)

Schwartz, S. E. 2007 Heat capacity, time constant, and sensitivity of earth's climate system. *J. Geophys. Res.* **112**, D24S05. (doi:10.1029/2007JD008746)

Stone, D. & Allen, M. R. 2005 Attribution of global surface warming without dynamical models. *Geophys. Res. Lett.* **32**, L18 711. (doi: 10.1029/2005GL023682)

Stott, P. A., Tett, S. F. B., Jones, G. S., Allen, M. R., Ingram, W. J. & Mitchell, J. F. B. 2001 Attribution of twentieth century temperature change to natural and anthropogenic causes. *Clim. Dyn.* **17**, 1–22. (doi:10.1007/PL00007924)

Stott, P. A., Jones, G. S. & Mitchell, J. F. B. 2003 Do models underestimate the solar contribution to recent climate change? *J. Clim.* **16**, 4079–4093. (doi:10.1175/1520-0442(2003)016<4079:DMUTSC>2.0.CO;2)

Stouffer, R. J. 2004 Time scales of climate response. *J. Clim.* **17**, 209–217. (doi:10.1175/1520-0442(2004)017<0209:TSOCR>2.0.CO;2)

Svensmark, H. & Friis-Christensen, E. 2007 Reply to Lockwood and Fröhlich—the persistent role of the Sun in climate forcing. Scientific report 3/2007, Danish National Space Center. See http://spacecenter.dk/publications/scientific-report-series/Scient_No._3.pdf/view.

Taylor, K. C. *et al.* 1997 The Holocene/Younger Dryas transition recorded at summit, Greenland. *Science* **278**, 825–827. (doi:10.1126/science.278.5339.825)

Tett, S. F. B., Stott, P. A., Allen, M. A., Ingram, W. J. & Mitchell, J. F. B. 1999 Causes of twentieth century temperature change. *Nature* **399**, 569–572. (doi:10.1038/21164)

Wetherald, R. T., Stouffer, R. J. & Dixon, K. W. 2001 Committed warming and its implications for climate change. *Geophys. Res. Lett.* **28**, 1535–1538. (doi:10.1029/2000GL011786)

White, W. B., Lean, J. & Cayan, D. 1997 A response of global upper ocean temperature to changing solar irradiance. *J. Geophys. Res.* **102**, 3255–3266. (doi:10.1029/96JC03549)

Wigley, T. M. L. 2005 The climate change commitment. *Science* **307**, 1766–1769. (doi:10.1126/science.1103934)

Wigley, T. M. L. & Raper, S. C. B. 1990 Climatic change due to solar irradiance changes. *Geophys. Res. Lett.* **17**, 2169–2172. (doi:10.1029/GL017i012p02169)

Wigley, T. M. L., Ammann, C. M., Santer, B. D. & Raper, S. C. B. 2005 Effect of climate sensitivity on the response to volcanic forcing. *J. Geophys. Res.* **110**, D09 107. (doi:09110.01029/02004JD005557)

Willis, J. K., Roemmich, D. & Cornuelle, B. 2004 Interannual variability in upper ocean heat content, temperature, and thermosteric expansion on global scales. *J. Geophys. Res.* **109**, C12 036. (doi:10.1029/2003JC002260)

Wolter, K. & Timlin, M. S. 1998 Measuring the strength of ENSO—how does 1997/98 rank? *Weather* **53**, 315–324.

Yu, H. *et al.* 2006 A review of measurement-based assessments of the aerosol direct radiative effect and forcing. *Atmos. Chem. Phys.* **6**, 613–666.